

# CHAPTER-3

# Armchair, Zigzag and Mixed Geometries of S-6C-4H-S

---

***In every instance of its application to date, the equations of quantum mechanics have yet to be shown to fail. There is, therefore, every reason to believe that an understanding of a great number of phenomena can be achieved by continuing to solve these equations.***

**- M.C. Payne**

We investigated ballistic transport properties of armchair (AC), zigzag (ZZ), mixed, rotated-AC and rotated-ZZ geometries of small molecules made of 2S, 6C & 4H atoms which exhibit  $sp-sp^2$  hybridization. The chains made of 6C-atoms with 1S-atom at each end and 4H-atoms attached to different C-atoms have been relaxed. This resulted in AC, ZZ, mixed geometry structures. Differences in Transmission coefficient (T) curves of AC, ZZ and mixed molecules suggest geometry dependence of conductance and are in accordance with the previously reported results for AC and ZZ nanoribbons. In addition, our computed results for rotated-AC and rotated-ZZ suggest that the angle between electrode surface layers and molecular axis play dominant role, compared to the role of angle between S-C bond and electrode surface layers, in determining conduction through the structure. The structures with molecular axis perpendicular to electrode surface layers yield higher conductance values.

## 3.1 Introduction

Due to their potential use in molecular electronic devices, electronic transport in organic molecules is one of the few fields that have been pursued immensely both experimentally and

computationally, in recent years [1]. Graphene sheets and nanoribbons are strong candidates for futuristic molecular electronics due to their tuneable and controllable properties that depend on its shape, surface termination, and applied field or pressure [2,3]. The exceptionally attractive features of their electronic and mechanical properties mainly depend on their electronic structure and geometry. In nanographenes, peripheral edges strongly affect the electronic states [4,5]. We were motivated to investigate the geometry-dependent transport properties of structures made of 6C-atoms, 2S-atoms at two ends, and 4H-atoms joined to four different C-atoms where  $sp$ - $sp^2$  hybridization is present. These chain structures arising from basic building block (namely benzene ring) of graphene and of nanoribbon have  $sp^2$  bonding for middle C-atoms and  $sp$  bonding for terminal C atoms. Benzene dithiolate is a very well studied structure, which can give common platform to the studies related to molecular conductance. This motivated us to choose chain structures made from 2S, 6C and 4H atoms. Each of the studied structures initially comprised of straight chain of 6C atoms with 4H atoms attached to four different C-atoms, and one S-atom at each end has been relaxed to get minimum energy structure. At the end of relaxation process, we get AC, ZZ and mixed (combination of AC and ZZ) geometries depending on initial positions of H-C bonding in the chain. Resultant geometries have energies very close to that of a benzene molecule. These chain structures are reproducibly synthesizable through computer simulation and have potential advantage over other nanoelectronic systems with tailored atomic configuration.

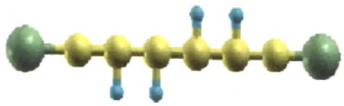
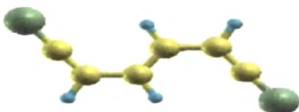
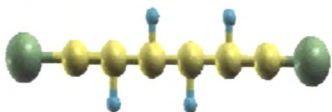
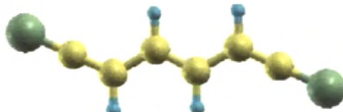
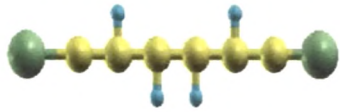
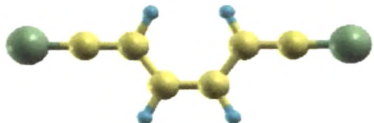
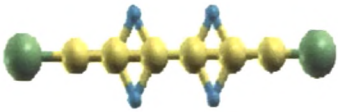
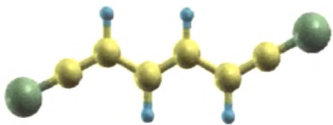
The substitution of S-atom at both ends of a chain has distinct effects. (a) It introduces new molecular states that are thiol (S) end-group related. (b) Conductance behaviour of different chain geometries is comparable, without concerning much about their mechanical properties, as thiol-electrode chemistry mainly determines the mechanical properties of junctions and is weakly dependent on the actual molecule between the electrodes [6]. (c) The Sulphur forms a

strong chemisorption bond with noble metal surfaces. We selected Al-nanorod as an electrode in place of widely used gold-nanorod. Gold has been suggested as one of the worst possible choices for high-conductance molecular nanowires as in the gold case the DOS of the leads does not penetrate into the molecule and electrons have to tunnel between both surfaces, which produces a very small zero-bias conductance [7]. The Al is noble metal having high conductivity and has been used in many prior performed benchmark calculations [5,8].

Three basic electronic processes in metal- molecule- metal junctions are; (a) charge transfer between the metals and the molecules, (b) change of the electrostatic potential and (c) modification of the molecular geometry and electronic states. The nature of these processes under both zero and nonzero bias determines the electrical characteristics of the molecular junction. In our case, device is at equilibrium and therefore the linear dc-transport properties of molecular device probes the equilibrium charge distribution of molecular junction established by adsorption of chains onto the electrodes. Therefore, there appears a need to determine the appropriate geometry of molecular junction and the resulting line-up of the molecular levels relative to the metal Fermi level, and modification of the molecular states. Solving of adsorption induced conformation change requires an accurate knowledge of surface lattice structure at the atomic scale for devices, which is not known in typical molecular transport measurement. Hence, one has to examine the effects that different adsorption and molecular geometries may have on the device characteristics. In view of this, we also computed conductance properties of 'rotated molecules' with respect to electrode surface layers.

### 3.2 Synthesis and Optimization of AC, ZZ and COMBO molecules

We first perform a structural optimization of every isolated molecule consisting of 6C, 2S and 4H atoms by relaxing until the forces are smaller than 0.025 eV/Å while keeping the large vacuum around them. The supercell size is kept more than 12 Å in  $x$  and  $y$  directions while more than 18 Å in  $z$  direction, so the molecules do not interact with periodic images formed in all three directions. The exchange-correlation energy is evaluated within Perdew and Zunger formula for local density approximation, which works relatively good in case of organic molecules, noble metals and alkali metals. Only valence electrons are explicitly considered using norm-conserving pseudopotentials to account for core-valence interactions. The kinetic energy cut off of 45 Ry is used for plane wave expansion of pseudo wave functions. The width of Gaussian type smearing has been chosen as 0.01 Ry for accurate energy band and density of state descriptions. Different molecules are prepared by taking into consideration the possible permutations of attaching 4H to chains made of 6C atoms and 2S atoms at end. These molecules made of 2S, 6C and 4H are chosen as benzenedithiolate is one of the most studied molecules for electronic transport. The molecular structures before and after the relaxation are shown in table 3.1. While benzene molecule can be viewed as cyclic trimer of acetylene, the relaxed chain geometries resemble with isomers of well-known conjugated  $\pi$ -electron polymer, polyacetylene. The AC geometry resembles with *cis*, ZZ geometry resembles with *trans* and MIXED geometry resembles with *trans-cisoid* isomers of polyacetylene.

No.	Initial geometry	Final Geometry	Structure Name
1			Armchair (AC)
2			Zigzag (ZZ)
3			Mixed (COMBO)
4			Zigzag (ZZ)

**Table 3.1:** Initial and final geometries of molecules made of 2S, 6C and 4H.

The geometry of a relaxed chain structure depends on where H-atoms are attached in the starting chain geometry. Accordingly, we get final geometries as armchair (AC), zigzag (ZZ) and mixed (COMBO) geometries as the final structures. The H atoms in initial geometry are at radial positions in cases like that shown in first row while at bridge position in other cases

such as in fourth row. However, final geometries for both the cases are identical. The S-C, C-C and C-H bond lengths for all molecules are given in table 3.2. Computed values of C-C bond length are in good agreement with those measured experimentally in polyacetylene [9] and with those calculated with density functional crystal orbital method using B3LYP functional [10].

Atoms Forming the bond	Bond lengths for molecules measured in Å		
	AC	COMBO	ZZ
S(1)C(1)	1.5415	1.5416	1.5421
C(1)C(2)	1.3213	1.3415	1.3222
C(2)H(1)	1.0991	1.1015	1.1017
C(2)C(3)	1.4406	1.4340	1.4320
C(3)H(2)	1.0976	1.0948	1.0976
C(3)C(4)	1.3552	1.3586	1.3564
C(4)H(3)	1.0977	1.0947	1.0976
C(4)C(5)	1.4399	1.4343	1.4323
C(5)H(4)	1.0993	1.1019	1.1015
C(5)C(6)	1.3216	1.3215	1.3222
C(6)S(2)	1.5414	1.5415	1.5422

**Table 3.2:** Computed bond lengths

### 3.3 Transmission co-efficient Calculations

A two-probe system is made of a central scattering region (also known as extended molecule) coupled with two atomic-scale Al [100] electrodes, which extend to reservoirs at  $\pm\infty$  where the current is collected. The electrode unit cell has two Al-atomic layers comprising of total 9 atoms. We took lattice constant and co-ordinates that of bulk Al-metal and the Al-Al bond length equal to 2.86 Å. Figure 2a and 2b show typical structures of central scattering region used in our investigations. In the central scattering region, a chain of 6C, 2S and 4H atoms couples with four surface layers of the left electrode and with three surface layers of the right electrode. Due to metallic screening in electrodes, charge and potential perturbations induced by chain adsorption extend only over a finite region of metal surface and these electrode surface layers in the central scattering region are large enough to ensure that the perturbation effects are screened and potential matches at junction of the scattering region and the electrode.

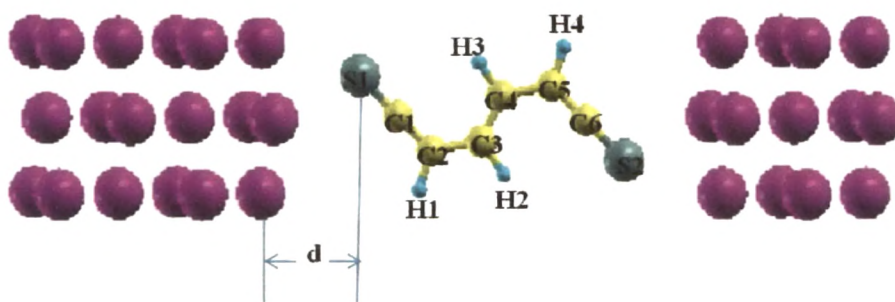


**Figure 3.1a:** The typical supercell used for calculation of conductance. Few layers of Al electrode (pink) on both sides of the AC molecule. There is sufficient vacuum of more than 9 angstrom in X and Y directions and it is periodic in Z- direction.

The central scattering region is confined into a periodic tetragonal supercell of sides  $a=b=13.23\text{\AA}$  (25 au) allowing for more than  $9\text{\AA}$  vacuum between the next periodic image in



the  $x$  and  $y$  direction [11] so that device does not interact with its mirror images. We computed the lattice parameter,  $c$  after optimization of distances between chains and the electrode surface layers. Here, we must notice that, T results with 3D electrode might be different.

During optimization of the distances between chain and the electrode surface layers, we kept the orientation of the chain axis perpendicular to the surface of electrode i.e. parallel to transport direction, while positions of both end S-atoms were kept symmetric with respect to surface of Al-electrodes. For AC molecule, we find that an optimal distance between surface layer of electrode and chain end atom,  $d$  is 2.8 Å, as is shown in Fig. 3.1a.

The value of  $d$  for both ZZ chain and mixed chain is found to be 2.6 Å. As has been reported in past, angle between chain axis and surface layers of electrode and the angle made by last atomic bond of chains (in our case S-C bond) with electrode surface layers are also of importance for computation of transport properties [12]. In view of this, we have also studied the effect of contact angle on the transmission coefficient values.

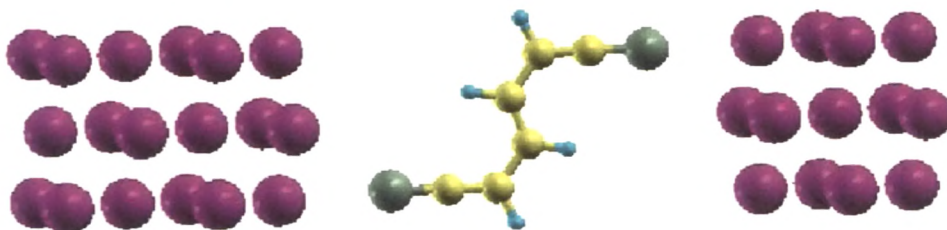


**Figure 3.1b:** The supercell same as in Fig.3.1a but having rotated-AC chain such that S-C bonds are perpendicular to respective electrode surface.

When the chain axis is perpendicular to the electrode surface layers, the S-C bond of AC-chain makes an angle of about  $45^\circ$  with the Al-surface, while that of ZZ- chain makes angle of about  $70^\circ$  and of both mixed chain and Benzene-molecule make an angle of about  $90^\circ$ . We

then rotated AC and ZZ chains in such a manner that the S-C bonds at both ends of chains get perpendicular to electrode surface layers. Fig. 3.1b display rotated AC chain.

Optimum distance,  $d$  between electrode surface layers and the rotated AC and rotated ZZ chains are equal to  $3.0 \text{ \AA}$  and  $2.7 \text{ \AA}$ , respectively. The position of atoms in scattering region is not relaxed after placing the chain between two electrodes, as additional effects introduced by relaxed positions of electrode atoms are avoidable for uniformity of electrodes, which is necessary for comparative study of different chains. To compare with ideal contact and know the electrode conductance behaviour, we placed Al-electrode unit cell as scattering region between two Al electrodes and got its conductance curve as shown in Fig. 3.2.

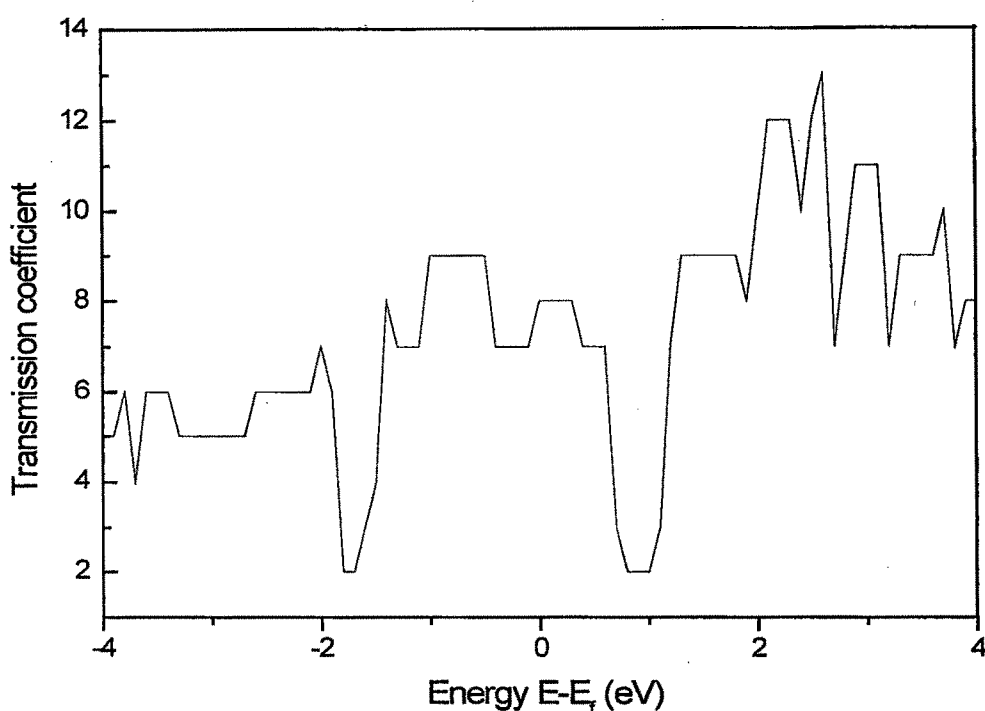


**Figure 3.2:** Transmission coefficient,  $T$  as a function of energy measured from Fermi energy set to zero, for the Al layers connected to Al electrodes (a case of ideal contact).

### 3.4 Results and Discussion

As is reported in table 3.2, length ( $\sim 1.32$  Å) of double bonds C1-C2 and C5-C6 is shorter than the ideal C-C double bond length ( $\sim 1.34$  Å) observed in alkenes. We can attribute this reduction in bond-length to the hybridization between C-orbitals. The  $sp-sp^2$  ( $sp^2-sp$ ) hybridization form double bond in case of C1-C2 (C5-C6), while in alkenes  $sp^2-sp^2$  hybridization forms the double bond. Similarly, for the single bond C2-C3 (C4-C5), bond length is  $\sim 1.43$  Å, which is smaller than C-C single bond length (1.53 Å) found in alkane. In our case, it is single bond between  $sp^2-sp^2$  C-atoms, while in alkanes, it is  $sp^3-sp^3$  single bond. Further, there is a resonance effect arising from the overlap of the p-orbital of a C-atom with the p-orbitals of its nearest neighbours on both sides. Therefore, an overlap between p-orbitals of C2-C3 and of C4-C5 bonds give them a double bond like nature to a certain extent and this could be a reason of decrease in bond length of C2-C3 and C4-C5, as compared to ideal single bond length. The resulting delocalization of the  $\pi$ -electrons makes chain more stable. Similarly, the resonance provides some degree of single bond character to C3-C4 double bond formed by  $sp^2-sp^2$  hybridization and it causes a decrease in bond length. The C-H distances observed in our relaxed chain structures are in the range of 1.097 Å to 1.102 Å, which is ideal for  $sp^2-s$  bond lengths.

We have computed transmission co-efficient (T) for benzene, AC, ZZ and mixed chains and have plotted them as a function of energy. Energy is measured in eV from Fermi energy set to zero. We computed T for per spin channel, as our electrode-chain-electrode system is non-magnetic. The total transmission co-efficient can be obtained by doubling our reported values of T. Several small sharp peaks, appearing in all transmission spectrums known as metal induced gap states (MIGS), do not belong to chain but have important impact on transport properties [12, 13]. In our case, investigated chains are short and their coupling with Al-electrode is very strong leading to larger hybridization with Al leads. Strong coupling between

the chain and two metal electrodes converts the discrete molecular levels to a continuous spectrum of density of states and a series of MIGS produced by hybridizations. This raises the peaks with long tails in density of state spectrum. The tails of frontier molecular levels (FMLs) and MIGS near Fermi level form the tunnelling regime in the spectrum. The magnitude and overlapping between tails of FMLs and MIGS influence the transmission coefficient.

On comparing our computed T for benzene, AC, ZZ, mixed, rotated-AC and rotated-ZZ chains with that of alkanedithiol of different length, we find that T-values of all chains are significantly larger than that of alkane molecules, reported in past [14]. The smallest alkane molecule, 2-alkanedithiol has height of tallest peak smaller than 0.4, in T-curve. While, our computed results for all chains having 6C atoms show peaks of height closer to 1.0. In addition to this, 6-alkanedithiol has maximum T-value up to 0.05, which is much smaller as compared to our computed T for any of the chains consisting of 6C atoms. We would however like to mention that metal electrode used in our calculation is different from that used in case of alkane molecules. As the MIGS play significant role in forming peaks in T, especially for shorter molecules, we can predict that coupling of molecules, studied by us, is stronger with Al-electrodes compared to coupling of alkanedithiol molecules with Au-electrodes. This suggests that Al can be proved a better electrode connecting to C-based short molecules.

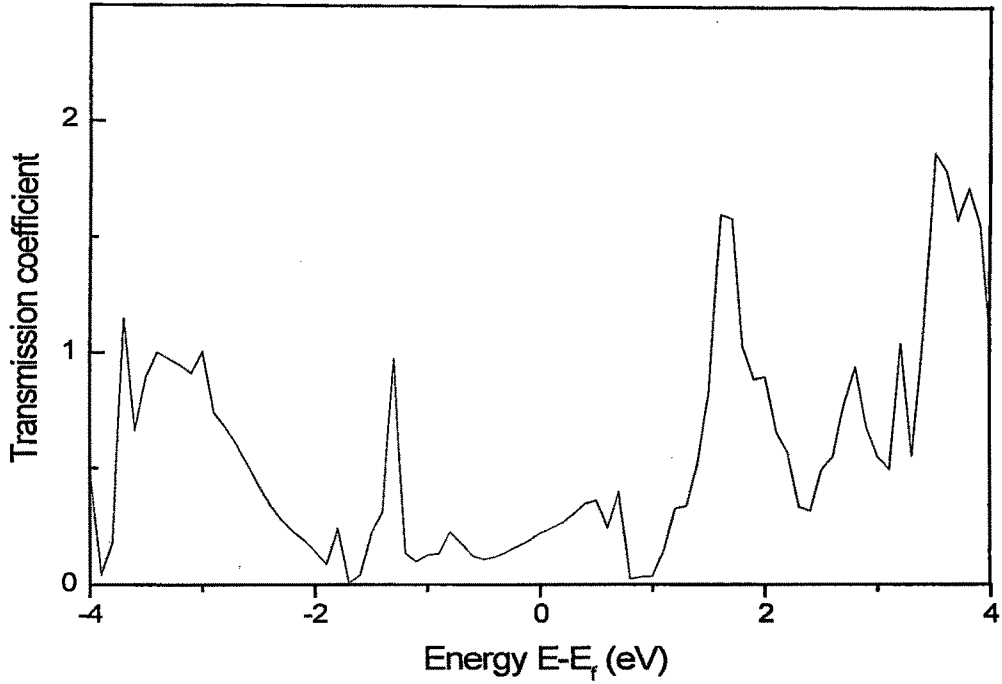


**Figure 3.3:** Transmission coefficient (T) for Benzene molecule as a function of energy measured from Fermi energy set to zero.

Looking at the results displayed in Fig. 3.3, we find that maximum value of T for benzene goes up to 1.8 along with other peaks values close to 1.4 and 1.2. These values of T are higher than the T-values for other chains reported in Figs. 3.4a, 3.5a, 3.6a, 3.7a and 3.8a. As is exhibited by Fig. 3.4a, the average height of peaks in T-curve for ZZ chain is close to one. We thus find that conducting nature of ZZ chain is in accordance with previously reported nature of Zigzag edged nanoribbons [15].

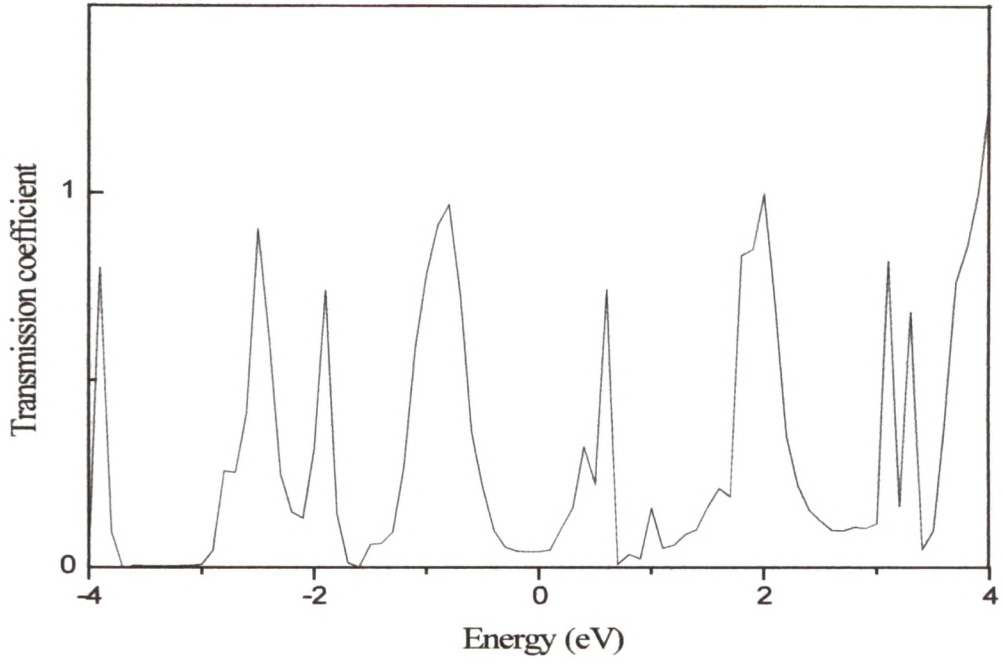


**Figure 3.4a:** Transmission coefficient (T) for ZZ chain as a function of energy measured from Fermi energy set to zero.

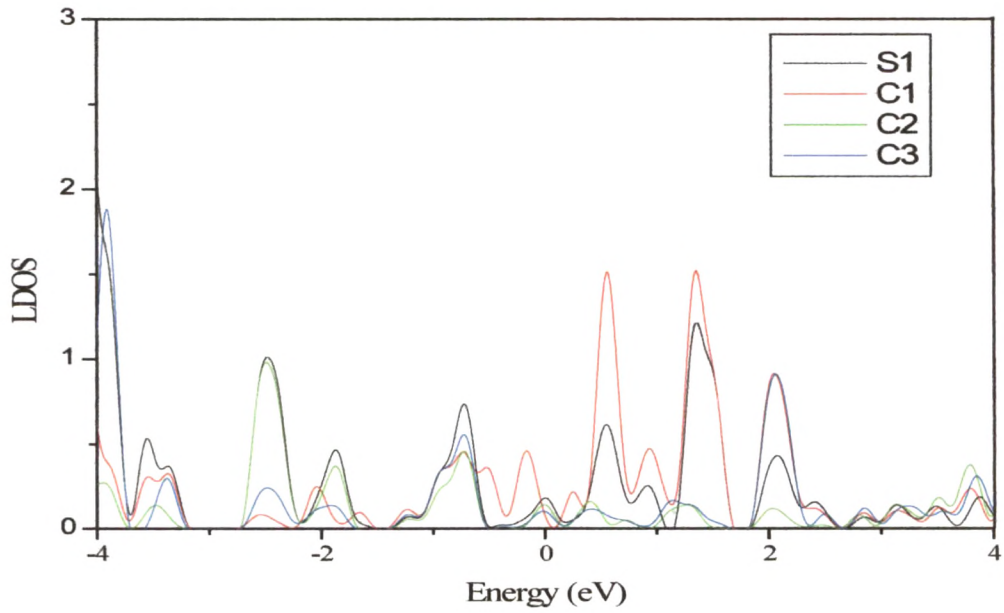


**Figure 3.4b:** The local density of states (LDOS) contribution by *P* orbitals of S1, C1, C2 and C3 atoms of ZZ chain connected to Al-electrodes are plotted as a function of energy measured from Fermi level. LDOS are in arbitrary units while energy is in eV.

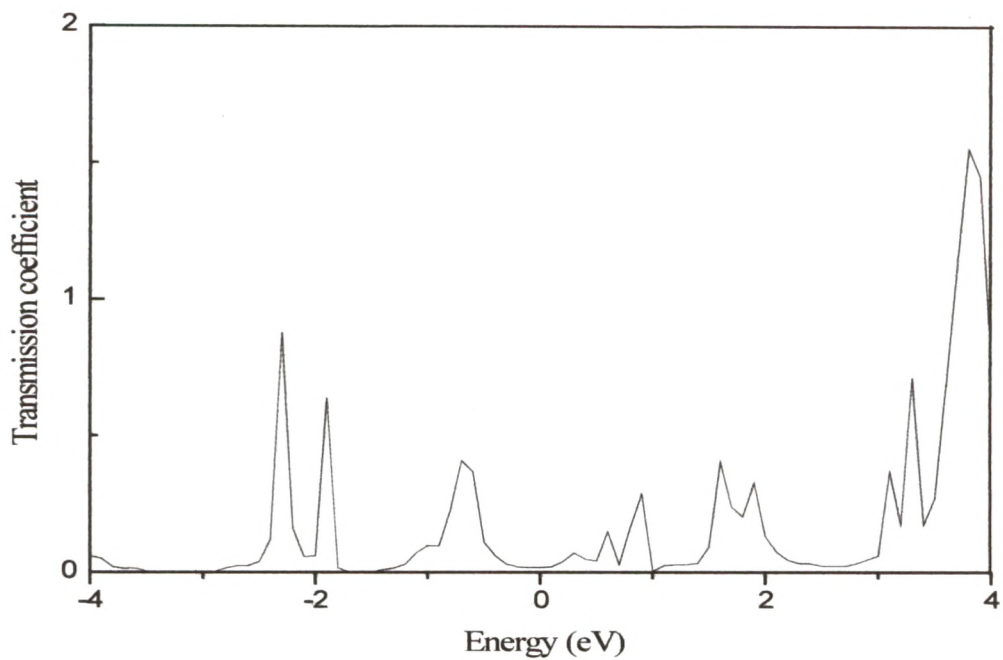


**Figure 3.5a:** The Transmission coefficient,  $T$  for AC chain as a function of energy measured from Fermi energy set to zero.

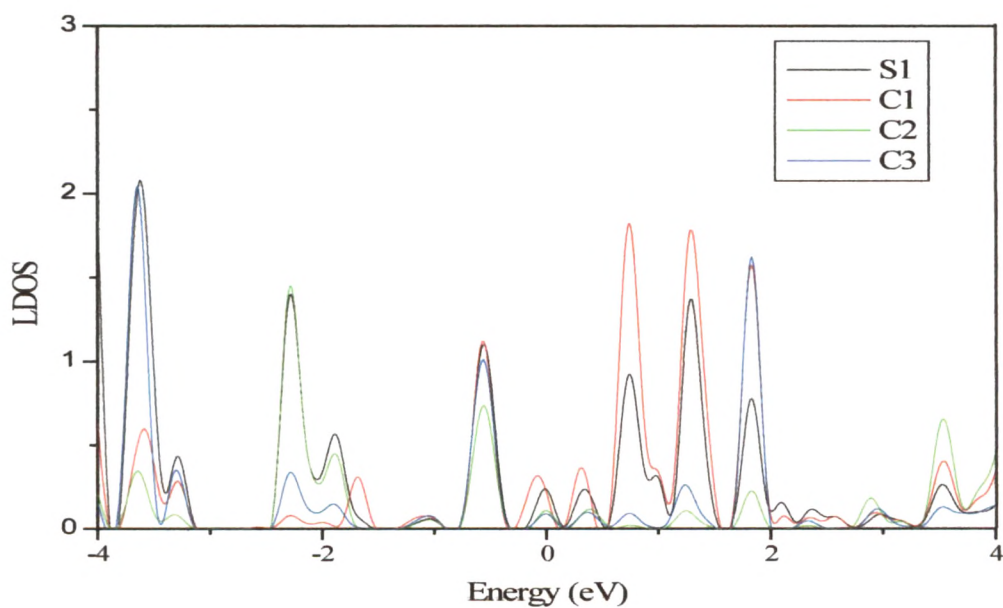


**Figure 3.5b:** The local density of states (LDOS) contribution by  $P$  orbitals of atoms marked as S1, C1, C2 and C3 in Fig.5 for AC chain connected to Al-electrodes are plotted as a function of energy measured from Fermi level. LDOS are in arbitrary units while energy is in eV.

The heights of different peaks in T-curve for AC chain are remarkably smaller, except one in the higher energy region, as is displayed in Fig. 3.5a. Thus, the average conductance of an AC-chain is lower than that of ZZ-chain, which has also been the case of conductance, reported for AC and ZZ nanoribbons [16-18]. Figs. 3.5a and 3.7a exhibit that the T for rotated-AC chain is much smaller in lower energy range as compared with that in higher energy range and the T-values for normal AC chain in the same energy range. However, rotation of AC chain does not affect the positions of peaks in T curve. On rotation of molecule, energy level matching gets perturbed and because of the change in degree of matching, eigen-channels that were conducting earlier do not contribute. For ZZ chain, optimized distance between the chain and electrode surface layers is 2.6Å, while in case of rotated-ZZ chain it is 2.7 Å. The angles made by S-C bond with electrode surface layers are 70° and 90°, respectively for ZZ and rotated-ZZ chains. Despite the changes in distance of chain from electrode surface layers and the angle between S-C bond and surface layer, peak positions and peak heights in T-curve for ZZ-chain are almost coinciding with those in T-curve for rotated-ZZ-chains, as is evident from Figs. 3.4a and 3.8a.

The above-mentioned observations, from our computed results, clearly suggest that the mechanism of conduction in armchair geometries differs qualitatively from that in zigzag geometries. In spite of changes in geometry and angle between S-C bond and electrode surface layer, the shape of T-curve for mixed chain is similar to that of ZZ chain, as is shown in Figs. 3.4a and 3.6a. The Eigen channel analysis shown in Figs. 3.4b and 3.8b indicate that, in the case of ZZ chain, number of eigenchannels contributing to T and hence the resultant T curve does not change on rotating the chain. However, in case of armchair geometries, number of eigenchannels and their contribution to T change on rotating the chain as is evident from Figs. 3.5b and 3.7b.



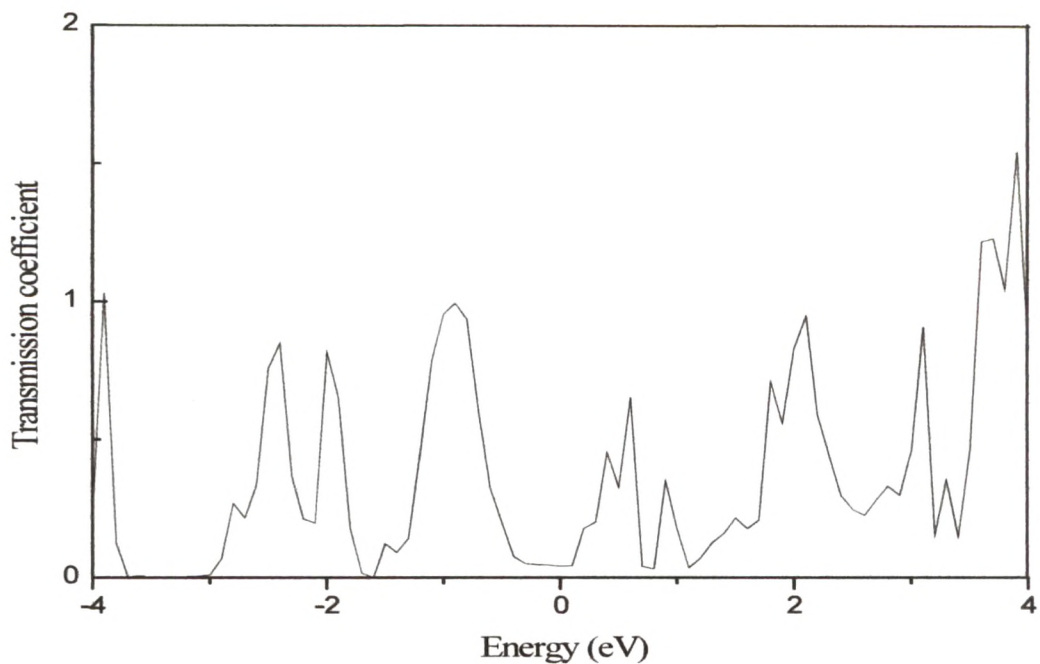


**Figure 3.6a:** The Transmission coefficient,  $T$  for mixed chain as a function of energy measured from Fermi energy set to zero.

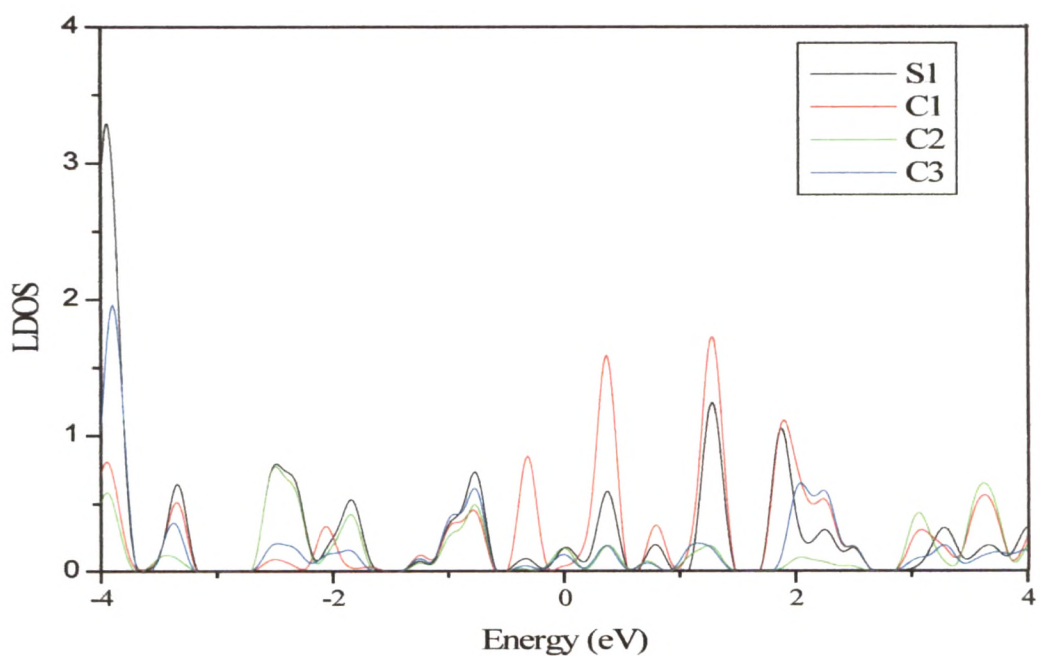


**Figure 3.6b:** The local density of states (LDOS) contribution by  $P$  orbitals of S1, C1, C2 and C3 atoms of mixed chain connected to Al-electrodes are plotted as a function of energy measured from Fermi level. LDOS are in arbitrary units while energy is in eV.

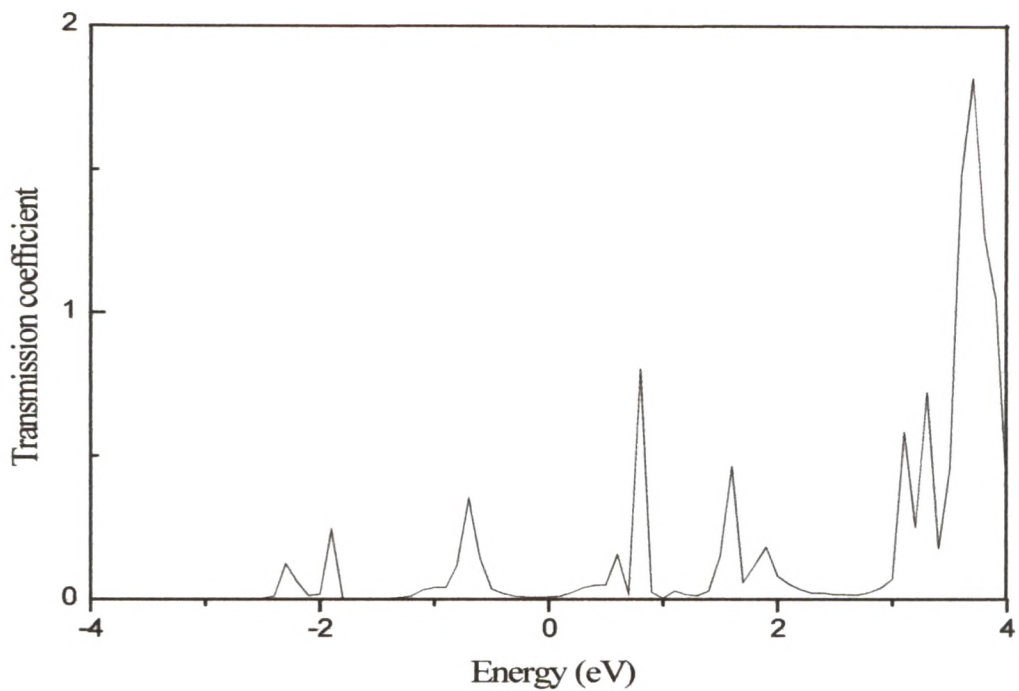


**Figure 3.7a:** The Transmission coefficient,  $T$  for rotated-AC chain as a function of energy measured from Fermi energy set to zero.

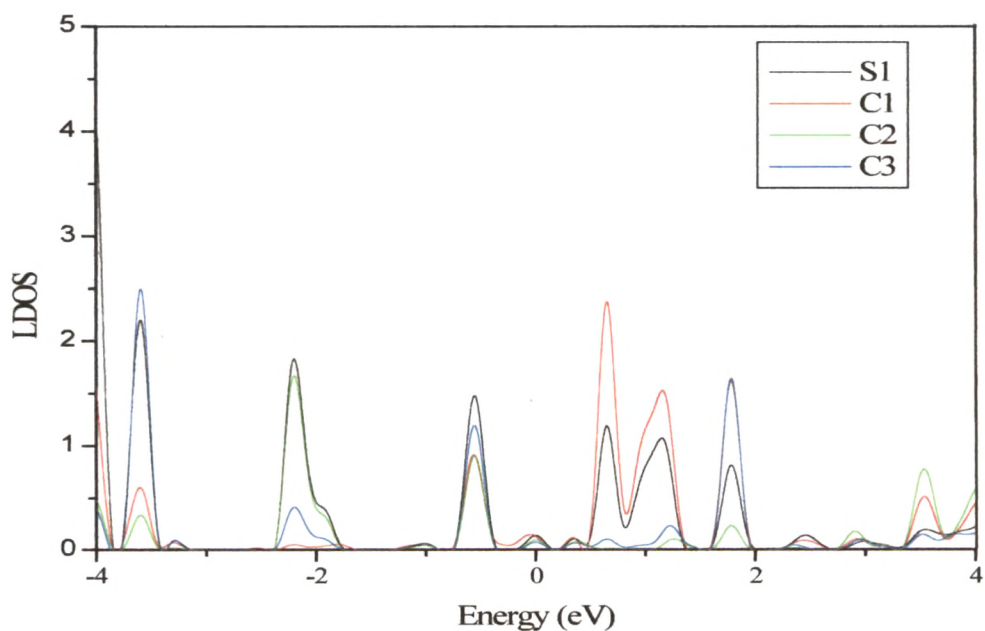


**Figure 3.7b:** The local density of states (LDOS) contribution by  $P$  orbitals of S1, C1, C2 and C3 atoms of rotated-AC chain connected to Al-electrodes are plotted as a function of energy measured from Fermi level. LDOS are in arbitrary units while energy is in eV.

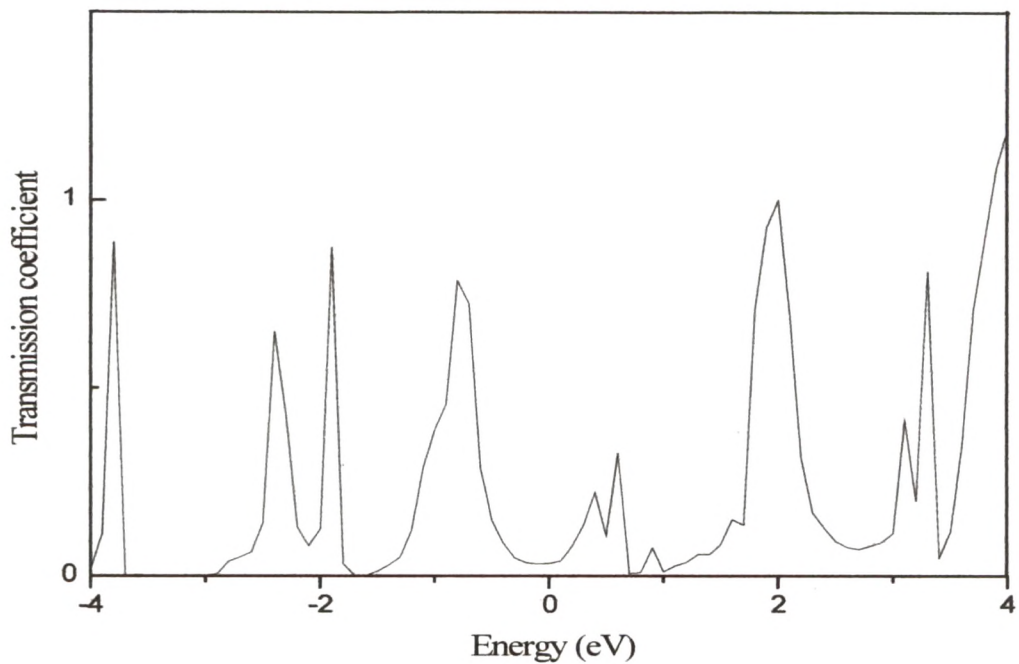


**Figure 3.8a:** The Transmission coefficient,  $T$  for rotated-ZZ chain as a function of energy measured from Fermi energy set to zero.

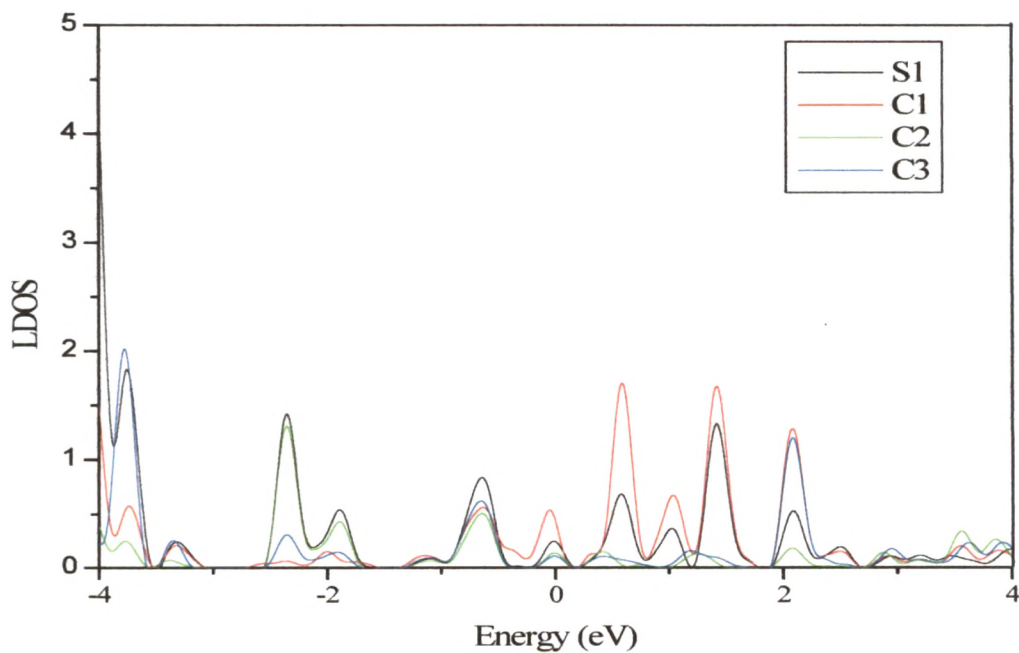
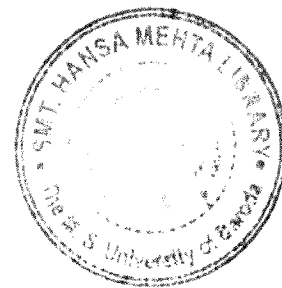


**Figure 3.8b:** The local density of states (LDOS) contribution by  $P$  orbitals of S1, C1, C2 and C3 atoms of rotated-ZZ chain connected to Al-electrodes are plotted as a function of energy measured from Fermi level. LDOS are in arbitrary units while energy is in eV.



Molecule	$G(E_f)$ in units of $G_0$
Benzene	0.22428
Zigzag	0.04252
Armchair	0.01756
Mixed	0.04158
Rotated Zigzag	0.03349
Rotated Armchair	0.00809

**Table 3.3: Computed Conductance for different molecules**

There have been several theoretical studies on absolute conductance for benzene molecule, with the reported values ranging from  $0.01G_0$  to  $0.5G_0$ [14, 15, 19]. Our computed value of equilibrium conductance at Fermi energy is,  $G(E_f) = 0.2243G_0$ . Table 3.3 displays our computed values of,  $G(E_f)$  for AC, ZZ and mixed chains. On comparing the value of  $G(E_f)$  for ZZ chain with that of rotated-ZZ chain, we find that  $G(E_f)$  of rotated-ZZ chain is nearly 21% lower than that of ZZ. While, rotated-AC chain yields 54% lower  $G(E_f)$  as compared to AC chain. We thus find that in rotated chain case, there is comparatively smaller contribution from MIGS. The main difference in geometries of normal and rotated chains is the angles made by molecular axis and S-C bond with electrode surface layers. In case of normal chains, the molecular axis is perpendicular to the surface layers, while in the case of rotated chains the S-C bond, at the end of chain, is perpendicular to the surface layers. In other words, for normal chain the molecule axis is in direction of transport, while in case of rotated molecule S-C bond is in the direction of transport. Our findings suggest that the angle between electrode surface layers and molecular axis play more important role, as compared to the angle between S-C bond and surface layers, in determining the conduction. Also, the

molecular axis must be perpendicular to surface layers to achieve better conductance values, otherwise MIGS contribution in HOMO-LUMO gap become smaller which tend to lower the conductance values near the Fermi level.

Local density of states (LDOS) contribution by  $P$  (sum of contribution by  $P_x$ ,  $P_y$ ,  $P_z$ ) orbitals of atoms marked as S1, C1, C2, and C3 in Fig.3.1a for ZZ, AC, mixed, rotated-AC and rotated-ZZ chains, connected to Al-electrodes, are plotted as a function of energy measured from Fermi level in Fig. 3.4b to 3.8b respectively. The molecular chains considered in our investigations are symmetric. Therefore, the LDOS curves for atoms marked as C4, C5, and C6 and S2 are similar to that of C3, C2, C1 and S1 atoms, respectively. In view of this, we computed LDOS for S1, C1, C2, and C3 atoms only. Comparing T-curves and LDOS curves, for each molecule, one can find close resemblance between peak positions of two curves. Contribution from S1 atom can be seen in all LDOS peaks of every atom. LDOS contribution from C1 atom is dominant in energy range from 0.5 to 1.5 above Fermi energy. C2 atom contributes dominantly for energies near 2 eV below Fermi energy. C3 atom contributes mainly for energies near 4 eV below Fermi energy and 2 eV above Fermi level. This tendency is followed in all molecular chains, though heights and widths of peaks vary for different molecular chains. For the peak at 0.75 eV below Fermi energy, all 4 atoms (S1, C1, C2 and C3) contribute to LDOS curve of all molecular chains and that peak is also seen in respective T curves. T-curves of all chains show dips near 1.8 eV below Fermi level and near 0.9 eV above the Fermi level. This is the effect of Al-electrode, which is evident from T-curve of Al-layers connected to Al-electrodes shown in Fig. 3.2.

### 3.5 Conclusion

We optimized different chain structures comprising of 6C, 4H and 2S atoms and get AC, ZZ and MIXED geometries resembling with *cis*, *trans* and *trans-cisoid* isomers of polyacetylene. The study of bond length between different C-C and C-H atoms suggest hybridization of orbitals and delocalization of electrons in these molecules. We computed T for all chain geometries made from 2S, 6C and 4H atoms. Our results suggest qualitative difference in conduction through armchair and zigzag structures, as has been the case with AC and ZZ nanoribbons. We conclude followings from our results on T: (i) Average conductance of an AC chain is lower than that of ZZ chain, which has also been the case of conductance reported for AC and ZZ nanoribbons. As earlier reported metallic nature of Zigzag edged nanoribbons, ZZ chain too is conducting. (ii) The T for rotated-AC chain is very small in lower energy range, as compared its values in higher energy regime and the T for normal AC chain. However, the positions of peaks remained unaffected on rotation of AC-chain structure. In spite of the changes in distance of chain from electrode surface layer and the angle between S-C bond and surface layers, the peak positions and peak heights in T-curve for ZZ chain almost coincide with those in T-curve for rotated ZZ chain. These observations clearly suggest that the mechanism of conduction in armchair geometries qualitatively differs from that in zigzag geometries. (iii) Though there is remarkable differences in the geometry, angle made between S-C bond and electrode surface layers, and the number of eigenchannels contributing to T, nature and shape of T-curve for mixed chain is almost identical to that for ZZ chain. (iv) Our findings suggest that the angle between electrode surface layers and molecular axis as compared to the angle between S-C bond and surface layers, play very important role in computing the conduction. In addition, molecular axis must be perpendicular to surface layers for achieving better conductance values.

### 3.6 References

- [1] R. Maul and W. Wenzel, Phys Rev B 80 (2009) 045424.
- [2] Pierre Darancet, Valerio Olevano, and Didier Mayou, Phys. Rev. Lett. 102 (2009) 136803.
- [3] Uwe Treske, Frank Ortmann, Björn Oetzel, Karsten Hannewald, Friedhelm Bechstedt, Phys Stat Sol (a) 207 (2010) 304.
- [4] Atsushi Yamashiro, Yukihiro Shimoi, Kikuo Harigaya, and Katsunori Wakabayashi, Phys. Rev. B 68 (2003) 193410.
- [5] Wei Fan, R. Q. Zhang, A. Reily Rocha, S. Sanvito, J. chem.. Phys. 129 (2008) 074710.
- [6] Ronaldo J. C. Batista, Pablo Ordejón, Helio Chacham, and Emilio Artacho, Phys. Rev. B 75 (2007) 041402(R).
- [7] V. M. García-Suárez and C. J. Lambert, Phys. Rev. B 78 (2008) 235412.
- [8] Brian Larade, Jeremy Taylor, H. Mehrez, and Hong Guo, Phys. Rev. B 64 (2001) 075420.
- [9] C. S. Yannoni and T. C. Clarke, Phys. Rev. Lett. 51 (1983), 1191.
- [10] So Hirata, Hajime Torii, Mitsuo Tasumi, Phys. Rev. B 57 (1998) 11994.
- [11] M.C. Payne, M. P. Teter, D.C. Allan, T. A. Arias, J. D. Joannopoulos, Rev. Mod. Phys. 64 (1992) 4.
- [12] Y. X. Zhou, F. Jiang, and H. Chen, R. Note, H. Mizuseki, and Y. Kawazoe, J. Chem. Phys. 128 (2008) 044704.
- [13] Ž. Crljen, A. Grigoriev, G. Wendin, K. Stokbro, Phys. Rev. B 71 (2005) 165316.

- [14] D. J. Mowbray, G. Jones, and K. S. Thygesen, *J. Chem. Phys.* **128** (2008) 111103.
- [15] C. Toher and S. Sanvito, *Phys. Rev. Lett.* **99** (2007) 056801.
- [16] A. N. Andriotis, Ernst Richter, Madhu Menon, *App. Phys. Lett.* **91** (2007) 152105;
- [17] Lian Sun, Yafei Li, Zhenyu Li, Qunxiang Li, Zhen Zhou, Zhongfang Chen, Jinlong Yang, J. G. Hou, *J. Chem. Phys.* **129** (2008) 174114;
- [18] Masayuki Yamamoto, Yositake Takane, and Katsunori Wakabayashi, *Phys. Rev. B* **79** (2009) 125421.
- [19] M. Strange, I. S. Kristensen, K. S. Thygesen, and K. W. Jacobsen, *J. Chem. Phys.* **128** (2008) 114714.